Computers, Materials & Continua
DOI:10.32604/cmc.2021.014404
Article

Tech Science Press

Nature-Inspired Level Set Segmentation Model for 3D-MRI Brain Tumor Detection

Oday Ali Hassen[1], Sarmad Omar Abter[2], Ansam A. Abdulhussein[3], Saad M. Darwish[4,*], Yasmine M. Ibrahim[4] and Walaa Sheta[5]

[1]Department of Computer Techniques Engineering, Imam Al-Kadhum College (IKC), Wasit, Iraq
[2]University of Information Technology and Communications, Media Technology Engineering Department, Iraq
[3]University of Information Technology and Communications, Baghdad, 10081, Iraq
[4]Department of Information Technology, Institute of Graduate Studies and Research, Alexandria University, 63 Horreya Avenue, El–Shatby, Alexandria, 21526, Egypt
[5]Informatics Research Institute, City of Scientific Research and Technology Applications, Borg EL Arab, 21934, Egypt
[*]Corresponding Author: Saad M. Darwish. Email: saad.darwish@alexu.edu.eg
Received: 18 September 2020; Accepted: 28 October 2020

Abstract: Medical image segmentation has consistently been a significant topic of research and a prominent goal, particularly in computer vision. Brain tumor research plays a major role in medical imaging applications by providing a tremendous amount of anatomical and functional knowledge that enhances and allows easy diagnosis and disease therapy preparation. To prevent or minimize manual segmentation error, automated tumor segmentation, and detection became the most demanding process for radiologists and physicians as the tumor often has complex structures. Many methods for detection and segmentation presently exist, but all lack high accuracy. This paper's key contribution focuses on evaluating machine learning techniques that are supposed to reduce the effect of frequently found issues in brain tumor research. Furthermore, attention concentrated on the challenges related to level set segmentation. The study proposed in this paper uses the Population-based Artificial Bee Colony Clustering (P-ABCC) methodology to reliably collect initial contour points, which helps minimize the number of iterations and segmentation errors of the level-set process. The proposed model measures cluster centroids (ABC populations) and uses a level-set approach to resolve contour differences as brain tumors vary as they have irregular form, structure, and volume. The suggested model comprises of three major steps: first, pre-processing to separate the brain from the head and improves contrast stretching. Secondly, P-ABCC is used to obtain tumor edges that are utilized as an initial MRI sequence contour. The level-set segmentation is then used to detect tumor regions from all volume slices with fewer iterations. Results suggest improved model efficiency compared to state-of-the-art methods for both datasets BRATS 2019 and BRATS 2017. At BRATS 2019, dice progress was achieved for Entire Tumor (WT), Tumor Center (TC), and Improved

Tumor (ET) by 0.03%, 0.03%, and 0.01% respectively. At BRATS 2017, an increase in precision for WT was reached by 5.27%.

Keywords: 3D-MRI tumor diagnosis; bio-inspired clustering; ABC optimization; multimodal detection

1 Introduction

The U.S. National Brain Cancer Society estimated that in 2017, 700,000 patients complained of a brain tumor, all of these patients may die [1]. The brain tumor is classified primarily into two major forms, a benign tumor, and a malignant tumor [2]. Diagnosing early-stage brain tumors will significantly affect chances for effective care and complete recovery [2,3]. Different tumor detection methods include brain biopsy and brain imaging systems [4,5]. Brain biopsy is a technique for grilling a cut in the skull and tissue and scraping the tumor for analysis. This is a risky, hazardous path to patient survival. Medical imaging methods have revolutionized tumor detection, helping physicians diagnose cancers quicker and boost prognosis. Recently, MRI has precise data such as tumor form, location, and scale. A patient's MRI is the screening of the human brain or three-dimensional brain anatomy. The MRI system can discern high-resolution soft tissue and becomes more alert, revealing slight differences in tissue density and tumor-related physiological changes [6]. Moreover, the lack of ionizing radiation by MRI allows it much more common among patients [7].

Brain tumor radiation therapy depends on accurate MRI segmentation requiring correct pixel labeling in MRI images as a tumor or healthy tissue [8]. The MRI modalities used in brain tumor segmentation and extraction are T1-weighted, T2-weighted, T1c, and Flair as T1c is counterbalance-enhanced, as well as flair is a fluid-attenuated reversal (see Fig. 1). Several cancers, including gliomas, also have fuzzy edges that are impossible to distinguish from healthy tissues. A multi-MRI series is commonly used as a remedy, supplying a special signature for any tissue type [9]. Segmenting tumor-bearing brain images is difficult for different reasons [9–11]. Original, high-grade gliomas (HGG) usually have undefined, irregular discontinuity limits, so it's debatable whether and how segmentation algorithms can handle the unthinkable part of the tumor. Moreover, tumor post-regions can only be separated if several modalities are integrated, enabling proper pre-processing registration. Finally, tumor identification is extremely challenging, since tumors differ greatly in size and position and have a variety of form and appearance properties. Finally, owing to the need for significant memory and computational assets, high-resolution MRI scanning can cause 3D segmentation problems [12]. Automated segmentation approaches are used to minimize the manually contouring frameworks' time-consuming task. If the object of concern becomes more homogenous and has irregular borders, the task becomes more challenging.

Volumetric images can provide accurate details in either direction rather than just a single view in a 2D view [13]. Numerous approaches were attempted to resolve the 3D MRI brain tumor segmentation problem. Two major methods exist to manage volumetric data. The first solution borrows the idea by real image segmentation, splitting 3D size into 2D slices and creating a 2D network that operates separately or deals simultaneously with each slice. The second approach is to crop volume patches and prepare a 3D network directly with volumetric patches. All approaches measure the original volume in a sliding window manner [14]. Due to the different resolutions in the MRI dataset's 3D space, 3D-MRI pre-processed into 2D slices, and axial slices are also used with most image segmentation as they have consistent dimensions (see Fig. 2). The second

approach utilizes level-set-based segmentation extensively. Fig. 3 shows a sample of 2D slice (T1c MRI) for brain tumor segmentation utilizing level set [15,16].

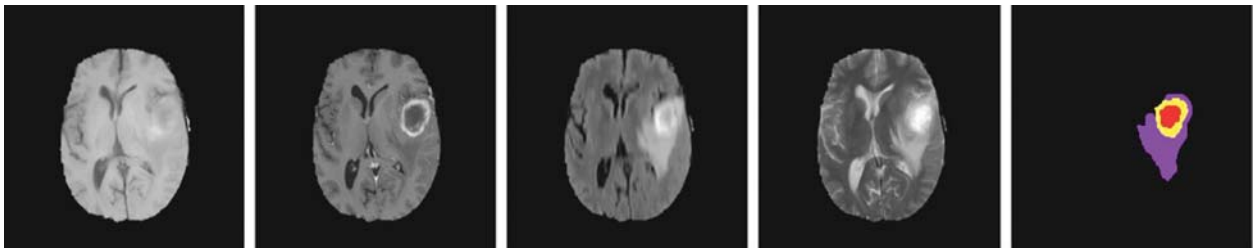

Figure 1: High-Grade Gliomas (HGG) BRATS axial slices subject: T1, T1c, T2-FLAIR, T2 and ground truth

Level-set-based segmentation offers a convenient way to determine the geometric characteristics of the evolving structure, and the fundamental benefit of using it is that it can represent complicated topology shapes and accommodate several topological changes, such as splitting and merging. Recently, an ABC optimization algorithm has been used to mimic the foraging action of honey bees with optimization problems [17–19]. The ABC offers successful search space exploration at exploitation expense. ABC's local search strategy relies on neighborhood search and greedy selection processes conducted by employed and onlooker bees. The ABC algorithm benefits from good robustness, rapid convergence, and high versatility. Nevertheless, it has drawbacks that include (1) Premature convergence in the later search time, (2) Very slow when used to solve hard search space problems [20].

1.1 Problem Statement and Motivation

Brain cancer has been one of the deadliest illnesses. An early cancer diagnosis is crucial to healing. Because as the human brain is so very complex, this region's tumor structure research is a complicated task. So, identifying brain tumors has become a difficulty. Present segmentation methods utilize different algorithms, such as threshold, model, and hybrid segmentation. These methods are sluggish and require the consumer to determine the initial contour, i.e., more mistaken. The motive for the work is to improve the physician's understanding of targeted artifacts (i.e., brain tumors); since this procedure has encountered several challenges, including lack of identification precision.

1.2 Aim of the Work and Contribution

This paper aims to provide an accurate brain tumor segmentation model that handles the drawback of current level set segmentation techniques. The suggested model combines Population-based Artificial Bee Colony Clustering (P-ABCC) and Level-set 3D-MRI scanning process. Utilizing the P-ABCC technique facilitates to extract level set' initial contour points accurately that helps to reduce the number of iterations and segmentation errors. Accurate segmentation of the brain helps doctors to the right choice and give great and right treatment. This strategy combines the k-means and the ABC algorithm. This integration is implemented through semantically fusing k-means clustering inside ABC. Instead of using random food sources (cluster centers) within ABC clustering; k-means regulates them accurately. The ABC module performance reflects the edges from all volume slices using the level set segmentation method.

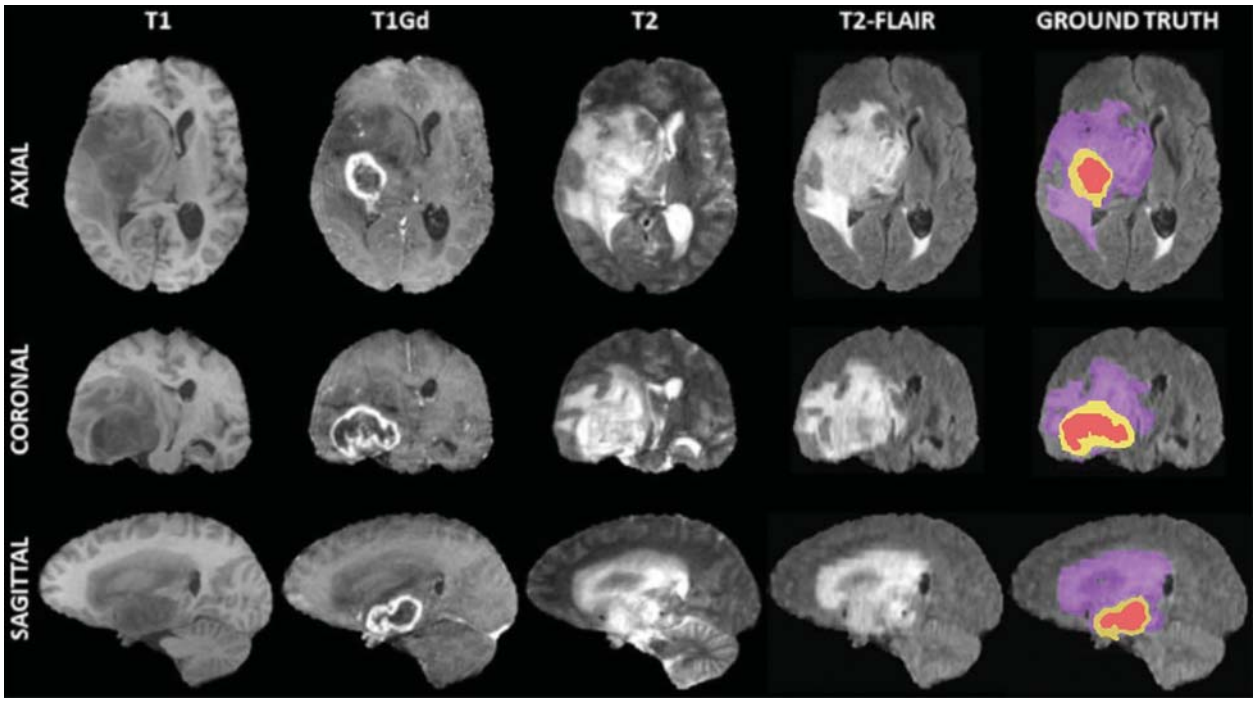

Figure 2: Example of one MRI slice from the BRATS challenge: From top to bottom three views (Axial, Coronal, and Sagittal)

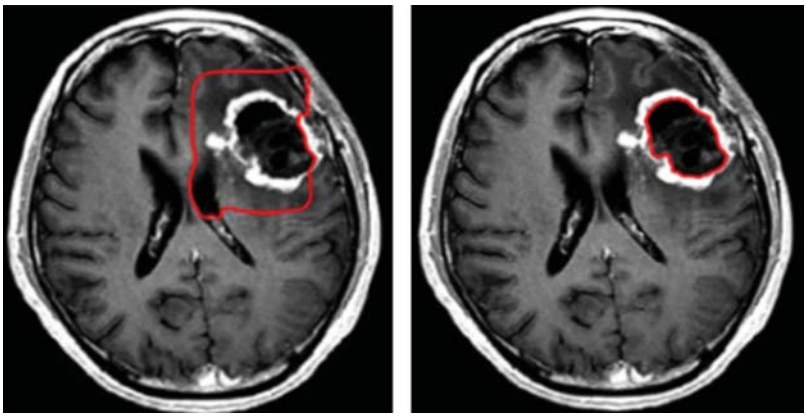

Figure 3: Example of level-set brain tumor segmentation

The rest of the paper is structured as follows: Section 2 describes some recent related work. Section 3 introduces the suggested 3D-MRI brain tumor detection model. In Section 4, the results and discussions on the BRATS' 2017 and BRATS' 2019 datasets are given. Finally, conclusions are drawn in Section 5.

2 Related Work

In particular, segmentation of brain algorithms could be narrowly divided into four main categories [21,22]: (a) Intensity-based segmentation which classifies individual pixels/voxels based upon their intensity; (b) Atlas-based segmentation which marks the desired biology or collection of anatomy by images produced by modalities of medical images; (c) Deep learning techniques that learn the associations between the pixels of input images by extracting representative features using convolution and pooling operations, (d) Model-based segmentation that involves the formulation of a propagating interface, and (e) Hybrid segmentation that integrates approaches to accomplish the segmentation target. Within the model- based segmentation type, the level-set approach allows segmentation easy to read forms that modify topology [23].

Over the past two decades, various approaches to tumor segmentation have been developed [9], typically categorized into two categories, one-modality, and multimodality-based. In [24], the authors introduced a level-set signed function for single-modality MRI tumor segmentation. This approach works well, even though the image is inhomogeneous. However, the model operates for the 3D volume of all tumor areas, and the iteration number of the level set is large; thus time absorbs. The principle of symmetry research was used in [25]; the authors suggested a system of 3D-MRI brain tumor identification focused on symmetry research using fast-bounding box methodology, accompanied by region-growing and geodesic-level approaches to acquire the initial tumor. This technique is useful and totally unsupervised and needs no training process. The disadvantages to this strategy are that populations with very limited tumor size, and multiple tumors have not been tested; authors also only segment the whole tumor.

In addition, a number of studies have been introduced that use a hybrid approach to brain tumor segmentation. In [26] the authors contributed a robust system the uses adaptive k-means for brain MRI segmentation. This kind of segmentation overcomes the k-means clustering restrictions, which create high sensitivity to the outer edge and noise. In the same direction, the authors in [27] introduced a hybrid brain tumor segmentation technique that uses k-means clustering and level sets to track the level set segmentation problems like poor convergence towards the tumor boundary and attraction towards false image features. The drawback of this approach is that due to random centroid initialization, k-means clustering is vulnerable to outliers as well as noise.

The authors in [28] merged k-means clustering and fuzzy c-means, and active level contour system in an integrated brain tumor segmentation process. Using intensity adjustment improves classification accuracy. The scholars used the same term in [29] and contrasted their findings with other clustering techniques. In addition, in [30], the scholars strengthened the approach by adding an extra layer focused on a mixed collection of image processing algorithms, whereas the other layers were centered on neural networks. Experimental results using this algorithm have shown that they can detect and identify the tumor accurately. Nevertheless, no examination was performed for numerous tumors.

Multi-modalities of MRI are commonly utilized in recent brain tumor classification. The authors developed a new multi-modal MRI-level-set segmentation of brain design in [31]. The pixels are divided into three types: tumor, edema, and T2 and T1c healthy brain tissue. The limitation of this method is the initialization of the level set contour as they involved the user in the initialization step of the segmentation process. Moreover, the authors in [32] suggested a new model for automated brain tumor segmentation using deep recurrent level sets. Nevertheless, in [33], the researchers implemented a modern technique using a Deep Neural Network (DNN) technique with a level-set mechanism for brain tumor sub-region segmentation. Throughout the

training process, they used DNN to identify the image core pixel with four material units (T1, T1c, T2, and flair). The DNN output is then used as a higher level-set initial contour. The level-set approach improves precision in segmenting MRI. DNN needs preparation in terms of training time, however.

The authors in [34] have used a feature representation learning technique to effectively discover local and conceptual knowledge from multi-modal brain images (T1, T1c, T2, and FLAIR). The limitation of this system is that it needs several labeled training data annotated by the nuclear fission of segmentation results from algorithms as well as clinical experts. Thus, resulting algorithms may skew the ground truth labels analytically. Similarly, the authors in [35] implemented an automatic brain tumor segmentation strategy in multimodal MRI by fusing the shape-based topology and Rough Fuzzy C-Means (R-FCM) algorithm to accurately detect brain tumor (ROI) region. The benefit of R-FCM is that it can better accommodate ambiguity and overlap partitions in datasets. This procedure needs high calculation time, however, and experiments were performed on one type of tumor.

Recently, the concept of superpixel-based brain tumor segmentation has emerged in which the image has segmented to small partitions using linear iterative clustering [36]. This method produces superpixels based on two things: similarity in color pixels and proximity in the image plane by using clustering pixels. The authors in [37] offered a super-voxel 3D method for multimodal MRI tumor segmentation. A wide range of features including Gabor and statistical features are selected for each super-voxel to segment tumor into TC, edema, or healthy brain tissue. In [38], depending on the superpixel-based brain tumor segmentation, the authors used extremely random trees to identify each superpixel in tumor and non-tumor and compared it to SVM. Still, superpixel-based techniques have drawbacks, including determining the optimum size for superpixels is difficult, computational complexity is high, less efficient in detecting small lesion area. Finally, the output depends on the initial centroid selection. In recent years, Diffusion Tensor Imaging (DTI) studies have gained considerable interest from researchers and physicians as they provide useful perceptions and have the ability to better diagnose infiltrative cancer cells. DTI was used in [39] for whole-brain segmentation to distinguish tumor volumes of significance for eventual tumor classification.

Today, considerable attention is given to utilizing bio-inspired optimization algorithms to segment medical images. For example, in [40], the authors contributed a new ABC-based brain tumor segmentation strategy. This model was compared on MRI images taken from a patient at multiple locations using k-means, FCM, as well as other genetic algorithms. Results showed that the ABC algorithm segmentation method gains both the best results visually and mathematically. ABC is poor at exploitation and its speed of convergence is an issue, and initial cluster centers are selected randomly. As described in [41], a novel integration of a fuzzy K-means (FKM) with an optimization technique is implemented to process MR images. The updated fuzzy k-means algorithm (MFKM) dependent bacteria foraging optimization (BFO) is built and proven to take minimal computational time in handling MR image sequences. MFKM identifies the segmentation mechanism and the BFO algorithm operates on optimum threshold values. Another analysis merged the ABC algorithm with the clustering algorithm for MRI image segmentation. Generally, meta-heuristics' usefulness depends primarily on encoding applicant solutions and thus the search room. The MRI brain tumor segmentation using the cuckoo search optimization algorithm was also considered.

In summary, level-set methods were shown to be versatile, effective, precise, and productive methods for a large range of medical image processing problems, especially MRI segmentation.

These approaches can manage jagged corners in the propagating solution, as well as topological and multidimensional affects. The drawback to level-set strategies is that extensive consideration is required to establish appropriate velocities to progress the level-set process. Nevertheless, little attention has been paid to creating a new nature-inspired clustering technique to tackle the downside of the existing level set detection techniques. Those techniques mainly rely and focus on a 3D-MRI brain tumor image.

3 Proposed Model

The contour should be adequately established to reliably diagnose a 3D-MRI brain tumor. The suggested model incorporates the level set segmentation and ABC optimization in order to achieve this objective. Herein, the P-ABCC is implemented through semantically fusing k-means clustering inside ABC. Instead of using random food sources (cluster centers) within ABC clustering; k-means regulates them accurately. The ABC module performance reflects the edges used as a greater focus for the level-set segmentation process. Fig. 4 displays the major model elements and how they've been interconnected. Our model uses local gray-scale attributes of FLAIR and T1c Visual representation of ideas as well as segments abnormal or tumor brain tissue in the form of whole-brain tumor, brain cancer core, and edema. The criteria for choosing T1c and FLAIR MRI methods is to use the same visual traits in brain tissues [9]. The suggested model can handle multi-sequence and multi-center MRI data [42]. Both the BRATS 2017 and BRATS 2019 datasets came from a variety of scanning instruments from 19 medical institutions (i.e., multi-center study). Each patient has four multi-sequence MRI images: T1, T1c, T2, and T2-FLAIR. Our model detects three tumor labels; WT and edema are detected using the FLAIR modality image while (TC and ET) are detected using T1c modality. The proposed method's segmented results are compared with the actual ground truth for brain WT, brain TC, and brain ET. Each following sections detail the major model elements.

3.1 Pre-Processing Phase

MRI images are commonly subject to various forms of noises, such as irregularities that may reduce the quality of the image [41]. In order to enhance MRI quality, the preprocessing procedure must be done both to improve image edges and, concurrently, to remove or decrease noise and to decrease any inhomogeneous regions of the image that leads to weak segmentation. In the proposed model, several steps had been adopted that include: Convert 3D-MRI into 2D slices, skulls stripping, anisotropic diffusion, and contrast enhancement. See [43,44] for more detail.

3.2 Population-Based ABC Clustering Phase

Clustering is an effective data processing method used to classify the collection of data items using a predefined criterion of similarity [45]. Many traditional clustering techniques do not perform satisfactorily in brain tumor segmentation scenarios due to a variety of reasons. See [46,47] for more details. ABC for clustering (ABCC) was influenced by bees' actions clustering purposes. The ABCC performs clustering based on random initial centroids, which are generated iteratively during the algorithm run. This excludes the algorithm from the clustering solution and renders a modest exploration. This study utilizes a modified ABCC called the population ABCC (P-ABCC) to address this issue. So, in our model, speed up convergence and balance between discovery and extraction, P-ABCC employs the k-means algorithm to enhance the ABC algorithm for clustering problems [46,47].

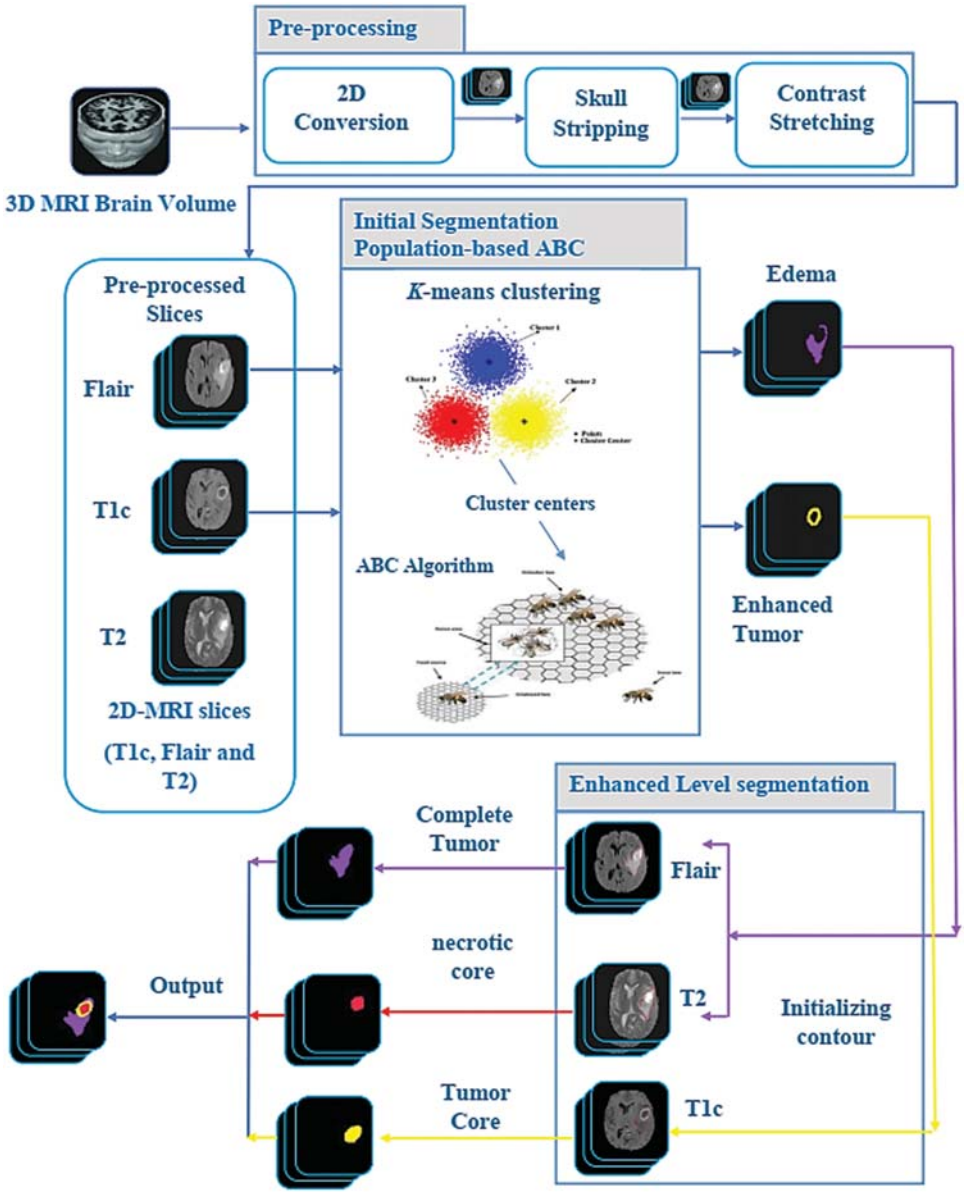

Figure 4: The proposed 3D-MRI brain tumor detection model

To tackle randomization to pick initial food sources (population) within the algorithm, k-means is used to generate an accurate food source. Applied clustering requires four stages: stage of initialization, stage of employed bee, stage of onlooker bee, and stage of abandoned food source and scout bee. The initial food source sites for employed bees are determined using the k-means method, instead of random food search. Stage of the employee bee is responsible for leveraging the newest food supply positions close to the old ones. The location of the new food source is defined by three items, the first item is an old food source location, the second is the bee position used, and the third element is a random variable within [0,1]. A probable value is then calculated for each food source relating to food source consistency. In the onlooker bee, a random

function is used to decide if the food source is nice or not to check for a new location of a food source. The current food source is abandoned if the user-defined limit parameter does not adjust the solution. First, the existing employed bees act as scouts, then the process of generating the new food source position. The method won't end before it passes a predefined criterion or end if the amount of iterations exceeds the limit. See [46–50] for the comprehensive details of each stage.

3.3 Level Set Segmentation Phase

Because of its consistency and irrelevance with topology, the level-set method shows a great advantage in solving edge-point problems and curve breaking [16]. However, this method includes various drawbacks. Because the edge-stop feature depends mostly on the gradient, only artifacts with Gaussian blur-defined edges may segment. Another drawback would be that in practitioners, the layer-stop function is never nearly zero at the edges, so the curve will surely reach object boundaries [16,51,52]. Moreover, when applying the level-set process, it is numerically essential to maintain the emerging level-set method near a signed width. Using the P-ABCC technique forced the level set function to be similar to a registered distance function, removing the need for expensive initialization. Here, the computed cluster centers for each slice will be used as initialization of the deformable model for final tumor segmentation. Hence, computation time is appropriate and computational efficiency is significant in terms of fewer iterations. Fig. 5 shows an example of level set-based brain tumor segmentation. See [51] for the formal definition of level set segmentation.

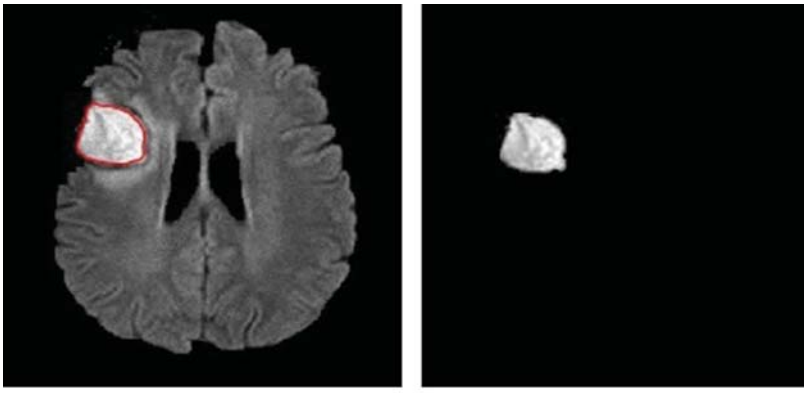

(a) (b)

Figure 5: Stem tumor segmentation with level collection (a) original image with initial contours (b) segmented tumor

4 Experimental Results

In this section, the output of the proposed model is validated with cerebral tumor MRI quantities, each representing a different tumor type, position, scale, and intensity. The experiment was performed in Intel (R), Core (TM) i3 CPU, 8.00 GB RAM implemented in MATLAB R2018a.These brain tumors image data were obtained from the segmentation challenge dataset that includes [53–55]: BRATS 2019 dataset: contains multi-institutional

preoperative (Multi-center) 3D-MRI of 336 heterogeneous (in shape, appearance, size, and texture) gliomas patients (259 HGG and 76 Low-Grade Gliomas LGG). Each patient in this dataset has 4 Multi-sequence MRI brain images: T1, T1c, T2, and T2-FLAIR. MRI data were captured with different clinical protocols and several scanners from 19 institutions. The output segmentation models can be tested in three tumor regions: (1) WT: hybrid of (edema + enhanced brain tumor + non − enhanced brain tumor + necrosis). (2) ET: Segmented improved brain tumor. (3) TC: (improved brain tumor + non − enhanced brain tumor + necrosis); [6,51,52]. BRATS 2017 dataset: were captured using several scanning instruments from 19 medical institutions. It includes 210 HGG with 75 LGG scans; already segmented results. Herein, we utilize the official evaluation metrics given by BRATS 2019: Dice score, Sensitivity (Recall), Specificity, and Hausdorff distance (HD) as evaluation metrics. Furthermore, accuracy and precision were used as evaluation metrics for BRATS 2017 dataset [53,56,57].

4.1 Qualitative Evaluation

The multi-modal MRI segmentation results of our proposed model on the BRATS 2019 segmentation challenge dataset are shown in Figs. 6 and 7. In these figures, the row represents one clinical case. In the four columns from left to right, images show one axial slice of MRI acquired in Flair, T1c and T2 modality, respectively, used as input to our model. In the fourth and the fifth columns, images show the GT and the prediction labels respectively, where tumor different regions can be notable by the following colors: peritumoral edema (purple), ET (yellow), and necrotic and non-ET (red). The combined tumor detection results shown in (Prediction) sensibly are similar to the ones obtained by the experts (GT). The same observation is shown in Fig. 8 for BRATS 2017 regarding detection of WT.

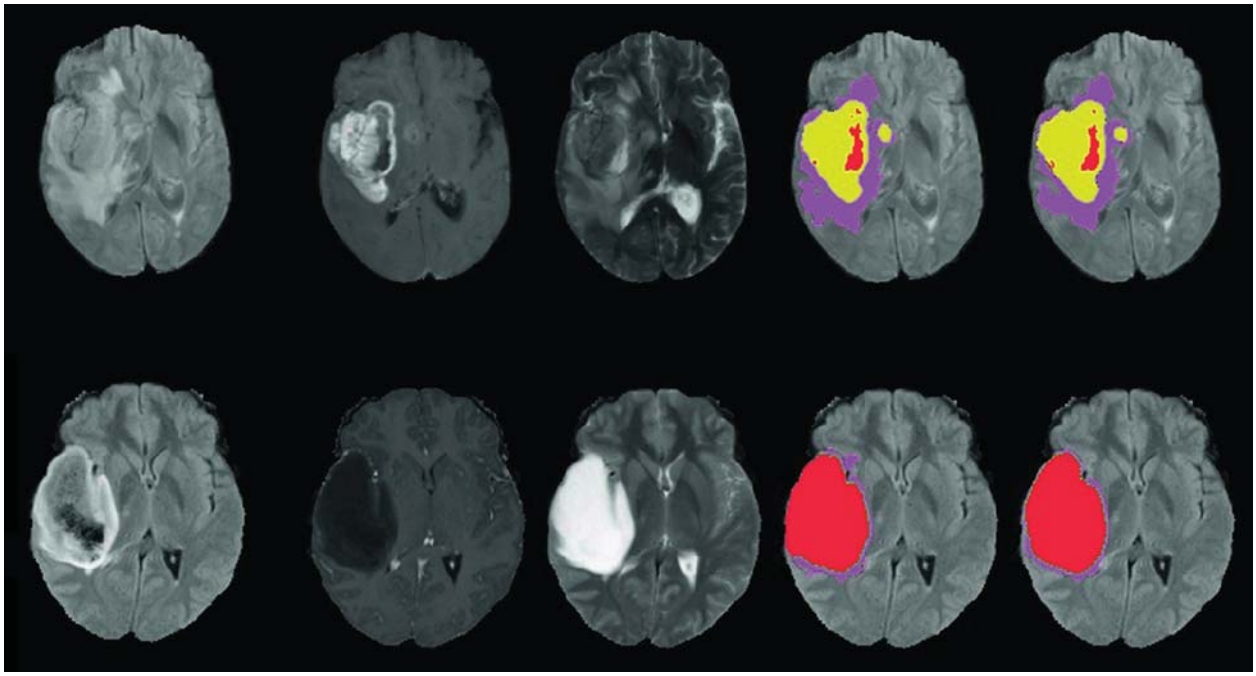

Figure 6: Example of two slices segmentation for BRATS 2019 from left to right: FLAIR, T1c, T2, prediction and ground truth

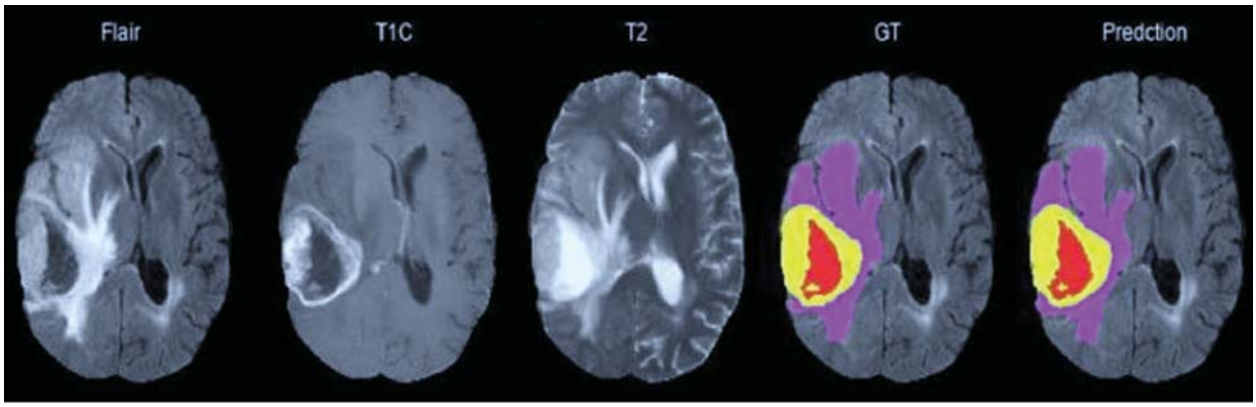

(a) (b) (c) (d) (e)

Figure 7: (a) FLAIR MRI modality (b) T1c MRI modality (c) T2 MRI (d) segmented edema in purple color, segmented enhancing tumor in yellow color and Segmented necrotic core in red color (e) ground truth

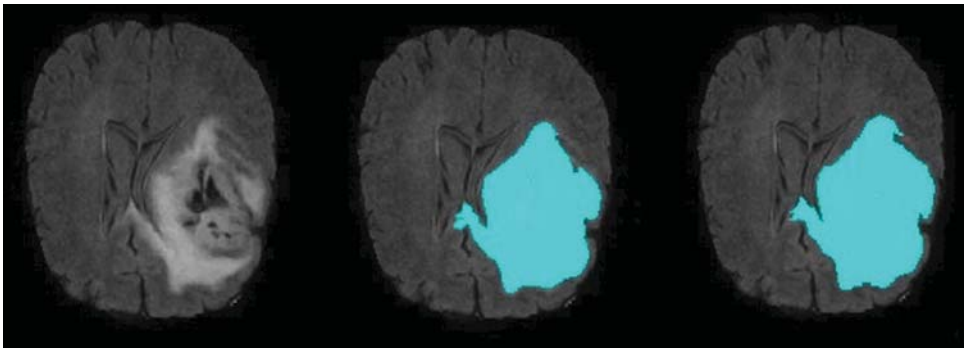

Figure 8: Example of one slice segmentation for BRATS 2017 data set, from left to right: FLAIR, prediction and ground truth

4.2 Quantitative Evaluation

4.2.1 Experiment 1: Model Performance for BRATS 2019 Dataset

For BRATS 2019 dataset, as pointed out in Tabs. 1 and 2, the value of the Dice ratio can exceed 0.93 for whole tumor segmentation, showing good overlap with manual segmentations. Also, in the same setting, sensitivity exceed 0.92. In terms of Specificity, the ratio is equal to 0.997 for the ET region. So, it means that the segmentation results are reliable enough.

4.2.2 Experiment 2: Comparison with Existing Machine Learning Methods for BRATS 2017 Dataset in Segmenting Whole Tumor

For the purpose of comparison with the suggested model, some related methods according to the published papers [25,27,32,35] were used for whole tumor segmentation on BRATS 2017 dataset. The default level-set parameters were assigned to the same values as in [58], where $\sigma = 1.5$, $\rho = 1$, $\epsilon = 1.5$, $\lambda = 5$ and the time step (∇t) is set 1 to assure the stability of the curve evolution, and the velocity term $\alpha = 15$. Tab. 3, Figs. 9 and 10 reveal the power of the suggested model

compared with other methods. One possible explanation of this result is that utilizing P-ABCC enhances the segmentation accuracy as it helps the level set procedure to start with an accurate initial contour instead of choosing it randomly or not accurate as the comparative methods work. The P-ABCC performs concurrently both global and local searches to find an optimal solution. The search mechanism of P-ABCC is maintained by the utilization of the information obtained from k-means. In other words, the connection between k-means and ABC helps to increase accuracy and decrease the error rate. On the opposing, as the initialization of ABC is done randomly so it can be trapped in local optima easily. Fig. 11 shows three examples of different tumor grades II, III, and IV, acquired using the FLAIR MRI protocol. In general, FCM, Rough-FCM, and k-means depend on the feature extraction module. The main issue in these methods is how to select the salient features. In addition, the region growing approach accuracy increasing relies on the initial seed points that are often obtained randomly.

Table 1: Evaluation results on BRATS 2019 dataset in terms of dice and sensitivity

	Dice			Sensitivity		
	WT	ET	TC	WT	ET	TC
Mean	0.936	0.760	0.851	0.924	0.765	0.831
St. Dev.	0.042	0.08	0.039	0.04	0.11	0.081
Median	0.94	0.78	0.94	0.910	0.743	0.79
25 quartile	0.89	0.71	0.89	0.771	0.71	0.78
75 quartile	0.98	0.79	0.98	0.953	0.79	0.92

Table 2: Evaluation results on BRATS 2019 dataset in terms of specificity and hausdorff95

	Specificity			Hausdorff95		
	WT	ET	TC	WT	ET	TC
Mean	0.994	0.998	0.997	5.408	3.401	7.357
St. Dev.	0.006	0.003	0.005	1.075	1.833	2.001
Median	0.995	0.999	0.999	3.124	5.221	3.877
25 quartile	0.993	0.998	0.996	4.00	4.441	3.871
75 quartile	0.997	0.999	0.999	5.661	6.330	5.407

Table 3: Comparison results of existing methods on BRATS 2017 dataset

Methods	Accuracy	Recall	Precision
Proposed model (P-ABCC, level set)	98.9	96.13	93.4
Symmetry analysis, level set [35]	93.63	89.00	N/a
FCM [35]	85.7	87.6	72.3
Rough-FCM [35]	N/a	90.0	92.0
k-means, level set [27]	89.3	92.7	75.8
DNN, level set [32]	91.0	96.0	93.0

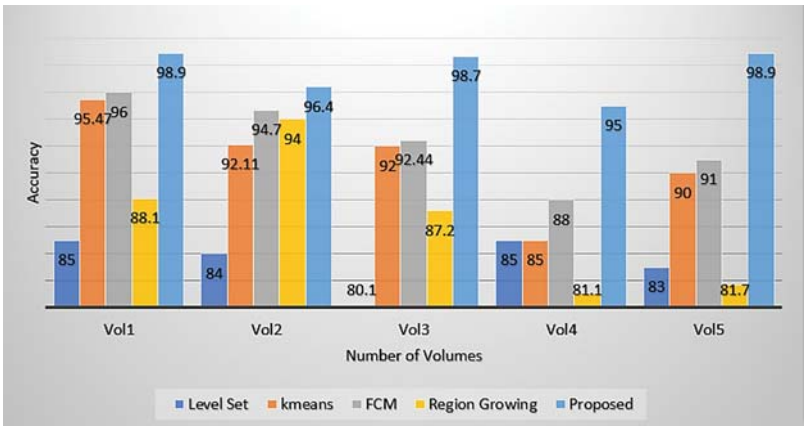

Figure 9: Comparison results of existing methods on BRATS 2017 dataset in terms of accuracy

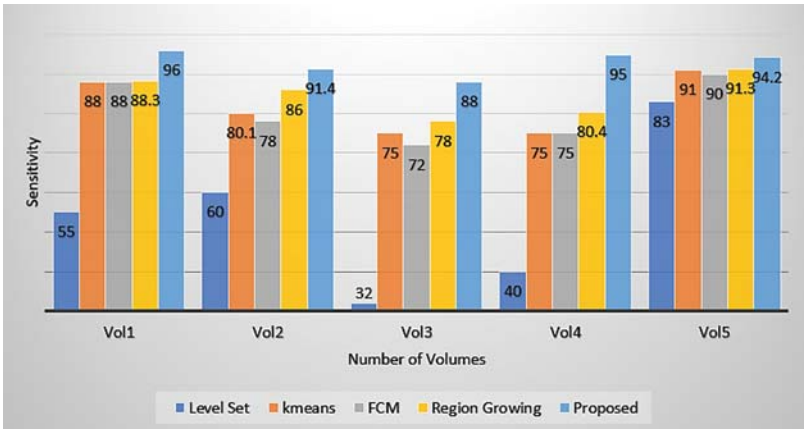

Figure 10: Comparison results of existing methods on BRATS 2017 dataset in terms of sensitivity

4.2.3 Experiment 3: Comparison with Superpixel-Based Segmentation Method for BRATS 2013 Dataset in Segmenting Different Parts of the Tumor

To confirm the efficiency of the proposed model compared to techniques that rely on the use of superpixel as one of the most famous tools for extracting brain tumors, another set of experiments was conducted to compare the proposed model with recent works in [38]. In this algorithm, the initial super-pixel centers are located by uniform sampling the pixels in one slice in 2D space. The search space is a square window with a size of two times more than a super-pixel size to decrease computations time. The cluster labels are altered for every iteration depending on the location and intensity distance of the pixels in the search area to the centers. The process is repeated until there is no new super-pixel with similar value to add to the ROI. However, this method lacks for segmenting TC region as it contains a limited super-pixel number.

Both methods are running on the BRATS 2013 dataset for tumor core, whole tumor and edema in terms of Dice score with 30 clinical (20 HGG) and (10 LGG) patient data. Tab. 4 shows a sample of the comparison results. The results confirm that the suggested model has better performance for both WT and TC by 0.01%, 0.5% respectively; yet it yields less performance

for edema by 0.02% compared with [38]. One possible clarification of this result is that the superpixel-based segmentation method initiates with initializing the superpixel seed positions to obtain the initial labels of pixels. So, the accuracy depends mainly on these seeds. Contrary to the proposed method, in which the seeds are identified in a way that makes them closer to real contour. Fig. 12 indicates qualitative comparison between the two methods according to manual segmentation methods.

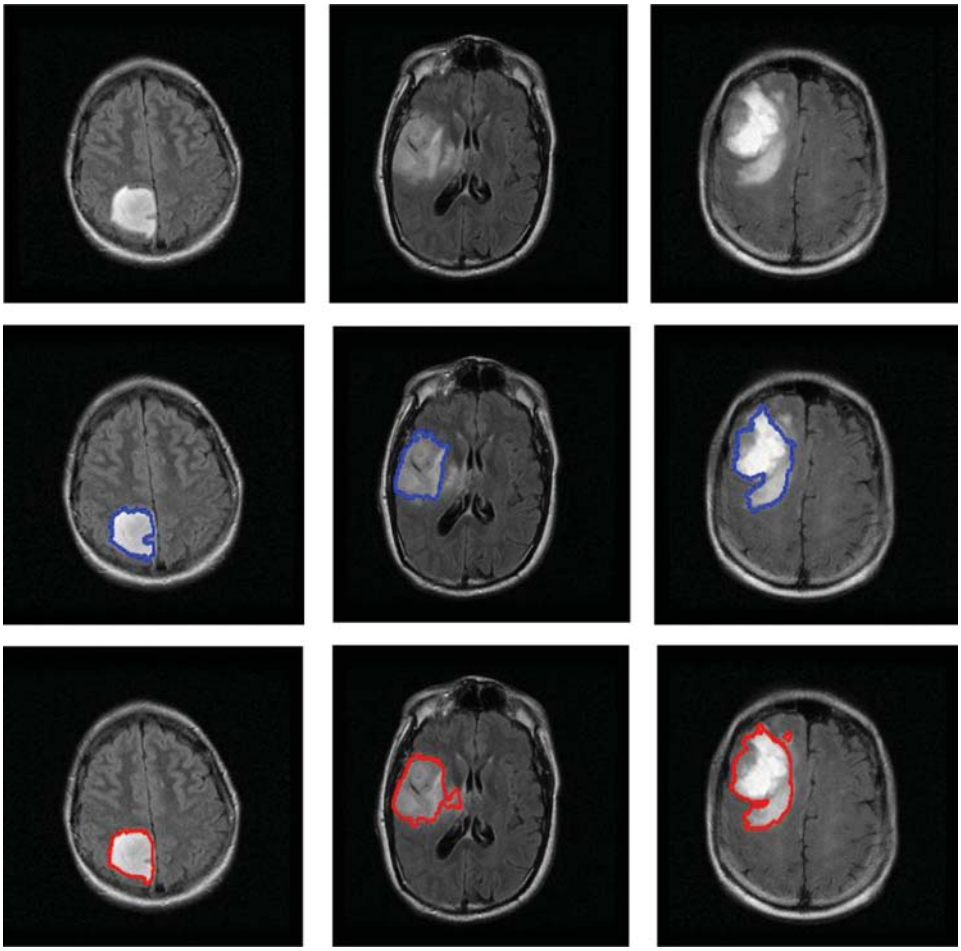

Figure 11: Example of Grade II, III, and IV brain oedemas: (upper row) original MRI slice, (middle row) modified level set segmentation, (lower row) manual segmentation

4.2.4 Experiment 4: The Effect of Using P-ABCC on Segmentation Accuracy for BRATS 2017 Dataset

This set of experiments was performed to compare the accuracy of the proposed model that employs P-ABCC to determine the initial contour and the traditional version of the model using ABC. The results shown in Tab. 5 revealed that the use of P-ABCC generates a further improvement of 7% for the same method with traditional ABC. The performance improvement comes from the correct and accurate classification as the P-ABCC procedure helps to enhance the detection accuracy of the tumor contour by choosing the initial seed as near as possible to the real contour.

Table 4: Dice score for the segmentation of edema, enhanced tumor and tumor core

Volume No	Super pixel [38]			Proposed model		
	WT	TC	Edema	WT	TC	Edema
1 (HGG)	0.77	0.84	0.69	0.97	0.86	0.87
2(HGG)	0.72	0.60	0.72	0.88	0.90	0.88
3(HGG)	0.72	0.68	0.70	0.90	0.88	0.90
4(LGG)	0.82	0.76	0.77	0.85	0.84	0.84
5(LGG)	0.83	0.62	0.83	0.88	0.84	0.88
Mean	0.89	0.80	0.89	**0.90**	**0.85**	**0.90**
STD	0.04	0.09	0.05	0.04	0.06	0.05

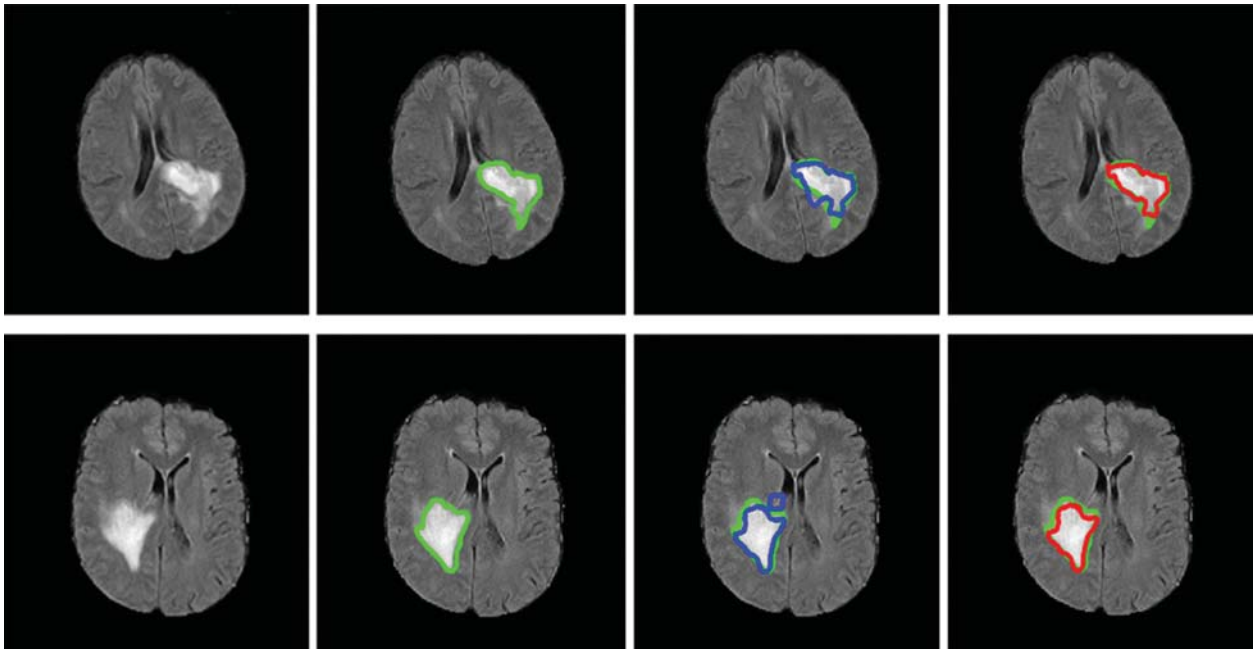

Figure 12: Examples of segmentation results overlay on manual segmentation (green) on BRATS 2013 data set. FLAIR image with tumor grade III (upper row), grade VI (lower row); (second column); manual segmentation; (third column) results using super pixel method; (Fourth column) results using the suggested model

Table 5: Comparison accuracy with and without P-ABCC on BRATS 2017 dataset for WT

Methods	Accuracy
Level set with P-ABC for clustering	98.0
Level set with ABC for clustering	91.67
Level set with ACO for clustering	91.65
Level set with PSO for clustering	91.95
Level set with CS for clustering	91.23

Furthermore, another subset of experiments was accomplished to verify the efficiency of the ABC for clustering for compared to other metaheuristics algorithms such as (a) Particle Swarm Optimization (PSO) algorithm, (b) Ant Colony Optimization (ACO) algorithm, and (c) Cuckoo Search Optimization (CS) algorithm [40,41,59]. We have replaced the P-ABC clustering module in the proposed model with a well-known optimization–based clustering as a Blackbox with their default configurations and the same fitness function. The results in Tab. 5 confirm that using P-ABC with level set segmentation will enhance, to some extent, the detection accuracy of brain tumors, compared with other different optimization methods for clustering; the increase of the accuracy for the P-ABC exceeds 7%. The results also confirmed that the type of metaheuristics algorithm used with level set segmentation has no role in increasing accuracy. This confirms the role of k-means as a selector for the initial population for ABC clustering and its significance to select the initial contour of the level set method as fairly close to the real boundary of (ROI) the tumor.

4.2.5 Experiment 5: Comparative Study on the BRATS 2019 Segmentation Challenge Dataset

To validate the efficiency of the suggested model on the BRATS 2019 dataset, some popular methods [60–63] that work on the same dataset were selected from the literature for comparison as shown in Tabs. 6 and 7. It can be easily found that in all performance metrics, the proposed approach outperforms all comparable methods. The worst performance in terms of the whole tumor is reported by [63] while for an enhanced brain tumor, the worst performance is reported by [62]. Among the compared methods, the performance of [61] is best in terms of the Dice score for an enhanced brain tumor. Our proposed model reveals the superiority in terms of Dice for the whole tumor and tumor core, yet it has less performance in the case of the Enhanced tumor while comparing to the represented model in [61]. As we can see, the specificity metric is nearly 1 (100 percent), meaning the two segmentations (ground truth and prediction) are about the same for this metric. We already noticed a decrease in Hausdorff distance. The first thing to conclude from this segmentation is that Glioblastomas brain tumors mostly contain one connected area, where we have seen an increase in segmentation performance. The second thing to conclude is that the ET class does not have many borders with the healthy tissue, and this indicates a decrease in the surface of the misclassified ET region and a good improvement in terms of Hausdorff distance metric.

Table 6: Evaluation results on BRATS 2019 training dataset in terms of dice and sensitivity

	Dice			Sensitivity		
	WT	ET	TC	WT	ET	TC
Model in [56]	0.905	0.764	0.820	0.910	0.771	0.825
Model in [60]	0.890	0.765	0.811	0.898	0.769	0.816
Model in [61]	0.896	**0.766**	0.790	0.913	0.768	0.777
Model in [62]	0.900	0.750	0.794	0.913	0.757	0.772
Model in [63]	0.894	0.737	0.807	0.897	0.766	0.826
Our model	**0.936**	0.760	**0.851**	**0.924**	0.765	**0.831**

Table 7: Evaluation results on BRATS 2019 training dataset in terms of specificity and hausdorff95

	Specificity			Hausdorff95		
	WT	ET	TC	WT	ET	TC
Model in [56]	0.994	0.998	0.997	5.408	3.402	7.375
Model in [60]	0.994	0.997	0.994	**5.381**	5.199	**7.243**
Model in [61]	0.993	0.998	0.997	6.900	4.600	8.400
Model in [62]	0.993	0.998	0.997	5.498	5.199	7.971
Model in [63]	**0.995**	0.998	0.996	5.677	5.994	7.357
Our model	0.994	**0.998**	**0.997**	5.408	**3.401**	7.357

4.2.6 Experiment 6: Role of P-ABCC to Reduce Level Set Iteration

The objective of this set of experiments is to verify the role of P-ABCC to reduce the computation cost of level-set segmentation with regard to iteration number required to find the final contour. The experiments were repeated 10 times to guarantee the robustness of the proposed model against random factors, which may affect the algorithm behavior. The ABC configuration parameters are regulated as colony size = 100, maximum cycles number = 20, and the number of clusters = 4 for five MRI volumes. It can be inferred from Fig. 13 that utilizing the ABC algorithm reduces the number of level set's iterations dramatically. By using the best configured P-ABCC parameters, the contour was figured very near to the tumor region.

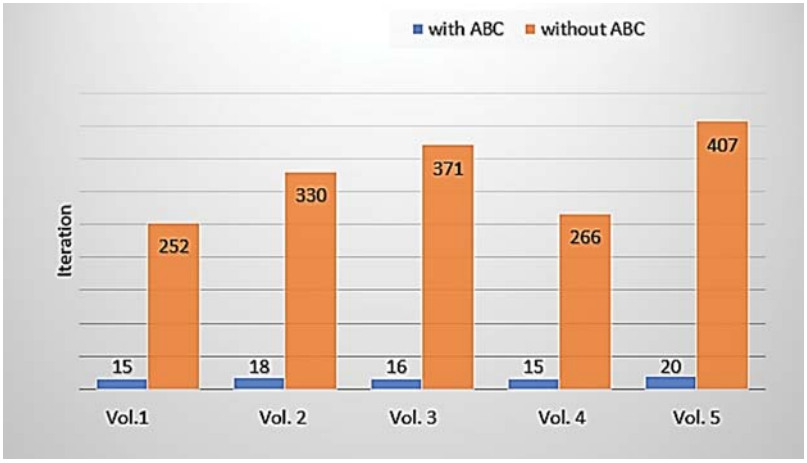

Figure 13: Level set iteration number for BRAT'S 2017 dataset

5 Conclusion and Future Work

This paper suggested an accurate model for segmenting tumors from 3D MRI medical images. The proposed model uses a level set segmentation technique that utilizing ABC-based clustering to regulate initial contour accurately instead of a random manner. The utilized bio-clustering algorithm employs k-means to select initial source food instead of random sources applied with

ABC with the aim of enhancing clustering accuracy. In other words, the suggested model handles two types of randomness; one within the ABC classifier by utilizing k-means, while the other one is within the level set procedures by utilizing two-steps ABC metaheuristic algorithm to select accurate level set' seeds points. The suggested model helps to extract accurate tumors instead of the commonly used trial and error contour detection methods. Also, it will help to extract the tumor's edge in a fast way by reducing the number of iterations in segmentation.

The experiments assessed the accuracy of our proposed model. Compared to the related work in terms of dice, sensitivity, and specificity measures on BRATS 2019 for both HGG and LGG clinical patient data, the proposed model demonstrates satisfactory performance with a slight increase in measurements by 0.031%, 0.12% for WT, TC respectively. Furthermore, for Hausdorff 95 measure, suggested model reveals reasonable performance with 0.1% increasing for ET; which highlights its ability to accurately determine the ET regions. Yet, on BRATS 2017, the suggested model achieves about a 5% increase in the segmentation accuracy of the WT. Future work includes utilizing the parallel segmentation approach to further decrease the complexity of the suggested model and enhancing its ability to deal with big data (multi-center studies).

Funding Statement: The author(s) received no specific funding for this study.

Conflicts of Interest: The authors declare that they have no conflicts of interest to report regarding the present study.

References

[1] M. El-Melegy, K. Abo El-Magd, S. Ali, K. Hussain and Y. Mahdy, "Ensemble of multiple classifiers for automatic multimodal brain tumor segmentation," in *Proc. of the Int. Conf. on Innovative Trends in Computer Engineering*, Egypt, pp. 110–114, 2019.

[2] M. Strong and J. Garces, "Brain tumors: Epidemiology and current trends in treatment," *Journal of Brain Tumors & Neurooncology*, vol. 1, no. 1, pp. 1–21, 2016.

[3] M. Nasor and W. Obaid, "Detection and localization of early-stage multiple brain tumors using a hybrid technique of patch-based processing, k-means clustering and object counting," *International Journal of Biomedical Imaging*, vol. 2020, no. 2, pp. 1–9, 2020.

[4] R. Aparna and P. Shanmugavadivu, "A Survey of medical imaging, storage and transfer techniques," in *Proc. of the Int. Conf. on Computational Vision and Bio-Engineering*, India, pp. 17–29, 2019.

[5] C. Lu, Z. Xu and X. Ye, "Evaluation of intraoperative MRI-assisted stereotactic brain tissue biopsy: A single-center experience in China," *Chinese Neurosurgical Journal*, vol. 5, no. 1, pp. 1–18, 2019.

[6] S. Bauer, R. Wiest, L. P. Nolte and M. Reyes, "A survey of MRI-based medical image analysis for brain tumor studies," *Physics in Medicine and Biology*, vol. 58, no. 13, pp. R97–R129, 2013.

[7] K. Mild, R. Lundström and J. Wilén, "Non-ionizing radiation in Swedish health care exposure and safety aspects," *International Journal of Environmental Research and Public Health*, vol. 16, no. 7, pp. 1186, 2019.

[8] Y. Zhuge, A. V. Krauze, H. Ning, J. Y. Cheng, B. C. Arora *et al.,* "Brain tumor segmentation using holistically nested neural networks in MRI images," *Medical Physics*, vol. 44, no. 10, pp. 5234–5243, 2017.

[9] J. Liu, H. Liu, Z. Tang, W. Gui, T. Ma *et al.,* "IOUC-3DSFCNN: Segmentation of brain tumors via IOU constraint 3D symmetric full convolution network with multimodal auto-context," *Scientific Reports*, vol. 10, no. 1, pp. 1–5, 2020.

[10] A. Işın, C. Direkoğlu and M. Şah, "Review of MRI-based brain tumor image segmentation using deep learning methods," *Procedia Computer Science*, vol. 102, pp. 317–324, 2016.

[11] J. J. Popoola, T. E. Godson, Y. O. Olasoji and M. R. Adu, "Study on capabilities of different segmentation algorithms in detecting and reducing brain tumor size in magnetic resonance imaging

for effective telemedicine services," *European Journal of Engineering Research and Science*, vol. 4, no. 2, pp. 23–29, 2019.

[12] M. Angulakshmi and G. G. Lakshmi Priya, "Automated brain tumor segmentation techniques-A review," *International Journal of Imaging Systems and Technology*, vol. 27, no. 1, pp. 66–77, 2017.

[13] S. Banerjee and S. Mitra, "Novel volumetric sub-region segmentation in brain tumors," *Frontiers in Computational Neuroscience*, vol. 14, no. 3, pp. 2481, 2020.

[14] S. Shirly and K. Ramesh, "Review on 2D and 3D MRI image segmentation techniques," *Current Medical Imaging Formerly Current Medical Imaging Reviews*, vol. 15, no. 2, pp. 150–160, 2019.

[15] S. Sajid, S. Hussain and A. Sarwar, "Brain tumor detection and segmentation in MR images using deep learning," *Arabian Journal for Science and Engineering*, vol. 44, no. 11, pp. 9249–9261, 2019.

[16] D. Wang, "Efficient level-set segmentation model driven by the local GMM and split Bregman method," *IET Image Processing*, vol. 13, no. 5, pp. 761–770, 2019.

[17] A. Geetha and N. Gomathi, "A Robust grey wolf-based deep learning for brain tumor detection in MR images," *International Journal of Engineering Education*, vol. 1, no. 1, pp. 9–23, 2019.

[18] H. Tsai, "Artificial bee colony directive for continuous optimization," *Applied Soft Computing*, vol. 87, pp. 1–30, 2020.

[19] B. Akay and D. Karaboga, "A survey on the applications of artificial bee colony in signal, image, and video processing," *Signal Image and Video Processing*, vol. 9, no. 4, pp. 967–990, 2015.

[20] A. Kumar, D. Kumar and S. Jarial, "A review on artificial bee colony algorithms and their applications to data clustering," *Cybernetics and Information Technologies*, vol. 17, no. 3, pp. 3–28, 2017.

[21] S. Saman and S. Jamjala Narayanan, "Survey on brain tumor segmentation and feature extraction of MR images," *International Journal of Multimedia Information Retrieval*, vol. 8, no. 2, pp. 79–99, 2018.

[22] A. Tiwari, S. Srivastava and M. Pant, "Brain tumor segmentation and classification from magnetic resonance images: Review of selected methods from 2014–2019," *Pattern Recognition Letters*, vol. 131, pp. 244–260, 2020.

[23] A. El-Baz and J. Suri, "*Level set method in medical imaging segmentation*," United States: CRC Press/Taylor & Francis, 2019.

[24] K. Thapaliya, J. Y. Pyun, C. S. Park and G. R. Kwon, "Level set method with automatic selective local statistics for brain tumor segmentation in MR images," *Computerized Medical Imaging and Graphics*, vol. 37, no. 7–8, pp. 522–537, 2013.

[25] A. Kermi, K. Andjouh and F. Zidane, "Fully automated brain tumor segmentation system in 3D-MRI using symmetry analysis of brain and level-sets," *IET Image Processing*, vol. 12, no. 11, pp. 1964–1971, 2018.

[26] V. Anitha and S. Murugavalli, "Brain tumor classification using two-tier classifier with adaptive segmentation technique," *IET Computer Vision*, vol. 10, no. 1, pp. 9–17, 2016.

[27] M. Krishnappa and D. Jayadevappa, "A hybrid approach for the segmentation of brain tumor using k-means clustering and variational level set," *Journal of Advanced Research in Dynamical and Control Systems*, vol. 10, no. 5, pp. 258–264, 2018.

[28] P. G. Rajan and C. Sundar, "Brain tumor detection and segmentation by intensity adjustment," *Journal of Medical Systems*, vol. 43, no. 8, pp. 430, 2019.

[29] E. Abdel-Maksoud, M. Elmogy and R. Al-Awadi, "Brain tumor segmentation based on a hybrid clustering technique," *Egyptian Informatics Journal*, vol. 16, no. 1, pp. 71–81, 2015.

[30] B. Ural, "A computer-based brain tumor detection approach with advanced image processing and probabilistic neural network methods," *Journal of Medical and Biological Engineering*, vol. 38, no. 6, pp. 867–879, 2017.

[31] Y. Song, Z. Ji, Q. Sun and Y. Zheng, "A novel brain tumor segmentation from multi-modality MRI via a level-set-based model," *Journal of Signal Processing Systems*, vol. 87, no. 2, pp. 249–257, 2017.

[32] T. Le, R. Gummadi and M. Savvides, "Deep recurrent level set for segmenting brain tumors," *Lecture Notes in Computer Science*, vol. 11072, pp. 646–653, 2018.

[33] P. Qin, J. Zhang, J. Zeng, H. Liu and Y. Cui, "A framework combining DNN and level-set method to segment brain tumor in multi-modalities MR image," *Soft Computing*, vol. 23, no. 19, pp. 9237–9251, 2019.

[34] C. Ma, G. Luo and K. Wang, "Concatenated and connected random forests with multiscale patch driven active contour model for automated brain tumor segmentation of MR images," *IEEE Transactions on Medical Imaging*, vol. 37, no. 8, pp. 1943–1954, 2018.

[35] A. Bal, M. Banerjee, A. Chakrabarti and P. Sharma, "MRI brain tumor segmentation and analysis using rough-fuzzy c-means and shape based properties," *Journal of King Saud University—Computer and Information Sciences*, vol. 30, pp. 1–19, 2018.

[36] M. Soltaninejad, X. Ye, G. Yang, N. Allinson and T. Lambrou, "Brain tumor grading in different MRI protocols using SVM on statistical features," in *Proc. of the Int. Conf. on Medical Image Understanding and Analysis*, UK, pp. 259–264, 2014.

[37] M. Soltaninejad, G. Yang, T. Lambrou, N. Allinson, T. Jones *et al.,* "Supervised learning based multimodal MRI brain tumor segmentation using texture features from supervoxels," *Computer Methods and Programs in Biomedicine*, vol. 157, pp. 69–84, 2018.

[38] M. Soltaninejad, G. Yang, T. Lambrou, N. Allinson, T. Jones *et al.,* "Automated brain tumor detection and segmentation using superpixel-based extremely randomized trees in FLAIR MRI," *International Journal of Computer Assisted Radiology and Surgery*, vol. 12, no. 2, pp. 183–203, 2017.

[39] T. Jones, T. Byrnes, G. Yang, F. Howe, B. Bell *et al.,* "Brain tumor classification using the diffusion tensor image segmentation (D-SEG) technique," *Neuro-Oncology*, vol. 17, no. 3, pp. 466–476, 2014.

[40] E. Hancer, C. Ozturk and D. Karaboga, "Extraction of brain tumors from MRI images with artificial bee colony-based segmentation methodology," in *Proc. of the 8th Int. Conf. on Electrical and Electronics Engineering*, Turkey, pp. 516–520, 2013.

[41] T. Dokeroglu, E. Sevinc, T. Kucukyilmaz and A. Cosar, "A survey on new generation metaheuristic algorithms," *Computers & Industrial Engineering*, vol. 137, pp. 1–29, 2019.

[42] F. Raschke, T. Barrick, T. Jones, G. Yang, X. Ye *et al.,* "Tissue-type mapping of gliomas," *Neuroimaging Clinical*, vol. 21, no. 101648, pp. 1–12, 2019.

[43] J. Iglesias, C.-Y. Liu, P. M. Thompson and Z. Tu, "Robust brain extraction across datasets and comparison with publicly available methods," *IEEE Transactions on Medical Imaging*, vol. 30, no. 9, pp. 1617–1634, 2011.

[44] R. Nair, E. David and S. Rajagopal, "A robust anisotropic diffusion filter with low arithmetic complexity for images," *EURASIP Journal on Image and Video Processing*, vol. 48, pp. 1–14, 2019.

[45] J. Chen and Y. Gong, "Particle swarm optimization for two-echelon location-routing problem," *Journal of Computer Applications*, vol. 33, no. 8, pp. 2261–2264, 2013.

[46] Y. Kumar and G. Sahoo, "A two-step artificial bee colony algorithm for clustering," *Neural Computing and Applications*, vol. 28, no. 3, pp. 537–551, 2015.

[47] G. Armano and M. R. Farmani, "Clustering analysis with combination of artificial bee colony algorithm and k-means technique," *International Journal of Computer Theory and Engineering*, vol. 6, no. 2, pp. 141–145, 2014.

[48] C. Zhang, X. Shen, H. Cheng and Q. Qian, "Brain tumor segmentation based on hybrid clustering and morphological operations," *International Journal of Biomedical Imaging*, vol. 2019, no. 3, pp. 1–11, 2019.

[49] A. Yurtkuran and E. Emel, "An enhanced artificial bee colony algorithm with solution acceptance rule and probabilistic multi-search," *Computational Intelligence and Neuroscience*, vol. 2016, no. 1, pp. 1–13, 2016.

[50] W. Gao, S. Liu and L. Huang, "A Novel artificial bee colony algorithm based on modified search equation and orthogonal learning," *IEEE Transactions on Cybernetics*, vol. 43, no. 3, pp. 1011–1024, 2013.

[51] C. Li, C. Xu, C. Gui and M. Fox, "Distance regularized level set evolution and its application to image segmentation," *IEEE Transactions on Image Processing*, vol. 19, no. 12, pp. 3243–3254, 2010.

[52] L. Zhong, Y. F. Zhou, X. F. Zhang, Q. Guo and C. M. Zhang, "Image segmentation by level set evolution with region consistency constraint," *Applied Mathematics-A Journal of Chinese Universities*, vol. 32, no. 4, pp. 422–442, 2017.

[53] S. Bakas, H. Akbari, A. Sotiras, M. Bilello, M. Rozycki Rozycki *et al.,* "Advancing the cancer genome atlas glioma MRI collections with expert segmentation labels and radiomic features," *Nature Scientific Data*, vol. 4, pp. 1234, 2017.

[54] K. Sharma, A. Kaur and S. Gujral, "Brain tumor detection based on machine learning algorithms," *International Journal of Computer Applications*, vol. 103, no. 1, pp. 7–11, 2014.

[55] B. Menze, A. Jakab, S. Bauer, J. Kalpathy-Cramer, K. Farahani *et al.,* "The multimodal brain tumor image segmentation benchmark (BRATS)," *IEEE Transactions on Medical Imaging*, vol. 34, no. 10, pp. 1993–2024, 2015.

[56] G. Cheng, J. Cheng, M. Luo, L. He, Y. Tian *et al.,* "Effective and efficient multitask learning for brain tumor segmentation," *Journal of Real-Time Image Processing*, vol. 2020, pp. 1–10, 2020.

[57] A. A. Taha and A. Hanbury, "Metrics for evaluating 3D medical image segmentation: Analysis, selection, and tool," *BMC Medical Imaging*, vol. 15, no. 1, pp. 178, 2015.

[58] K. Zhang, L. Zhang, H. Song and W. Zhou, "Active contours with selective local or global segmentation: A new formulation and level set method," *Image and Vision Computing*, vol. 28, no. 4, pp. 668–676, 2010.

[59] E. George, G. Rosline and D. Rajesh, "Brain tumor segmentation using cuckoo search optimization for magnetic resonance images," in *Proc. of the GCC Conf. & Exhibition*, Muscat, pp. 1–6, 2015.

[60] X. Cheng, Z. Jiang, Q. Sun and J. Zhang, "Memory-efficient cascade 3D U-net for brain tumor segmentation," *Lecture Notes in Computer Science*, vol. 11992, pp. 242–253, 2020.

[61] M. Hamghalam, B. Lei and T. Wang, "Brain tumor synthetic segmentation in 3D multimodal MRI scans," *Lecture Notes in Computer Science*, vol. 11992, pp. 153–162, 2020.

[62] M. Vu, T. Nyholm and T. Löfstedt, "TuNet: End-to-end hierarchical brain tumor segmentation using cascaded networks," *Lecture Notes in Computer Science*, vol. 11992, pp. 174–186, 2020.

[63] F. Wang, R. Jiang, L. Zheng, C. Meng and B. Biswal, "3D U-Net based brain tumor segmentation and survival days prediction," *Lecture Notes in Computer Science*, vol. 11992, pp. 131–141, 2020.